

Hybrid PWM Modulation Technology Applied to Three-Level Topology-Based PMSMs

Yuanxi Chen^{*}, Xinhua Guo[†], Jiangyu Xue^{*}, and Yifeng Chen^{**}

[†]*Department of Electrical Engineering, College of Information Science and Engineering, Huaqiao University, Xiamen, China

^{**}Xiamen EVADA Electronics Limited Corporation, Xiamen, China

Abstract

The inverter is an essential part of permanent magnet synchronous motor (PMSM) drive systems. The performance of an inverter is greatly influenced by its modulation strategy. Using a proper management of modulation strategies can guarantee high performance from a PMSM under various speed conditions. Switching between modulations is a pivotal technique that determines the performance of a PMSM. Most works on hybrid methods focus on two-level induction motors drive systems. In this paper, in order to improve the performance of PMSMs under various speed conditions, a hybrid method of a pulse width modulation (PWM) control scheme based on a neutral-point-clamped (NPC) three level topology was proposed. This hybrid PWM modulation comprised space vector PWM (SVPWM) and selective harmonic elimination PWM (SHEPWM). Under low speed conditions, the SVPWM is employed to cause the PMSM to start smoothly, and to obtain a rapid response from the control system. Under high speed conditions, the SHEPWM is employed to reduce the switching frequency and to eliminate particular current harmonics. Moreover, the harmonic characteristics of different modulations are analyzed to obtain a smooth transition between the SHEPWM and the SVPWM. Experimental and simulation results indicated the effectiveness of the proposed control method.

Key words: Modulation switch, NPC three-level, PMSM, SHEPWM

I. INTRODUCTION

Traditionally, a three-level topology is widely used for various applications, including the inverters and rectifiers in electrical energy conversion systems, since it can reduce the phase-current harmonics and switching frequencies, and withstand the voltage of the power device. The topologies of three-level inverters such as H-bridge-cascaded [1], [2], neutral-point-clamped (NPC) [3]-[5] and flying capacitors (FC) [6], [7] can substantially increase the efficiency of a system and reduce the stator harmonic current in motor drive systems [8]. The modulation mode of a three-level inverter can involve sinusoidal pulse width modulation (SPWM), space vector pulse width modulation (SVPWM) and selective

harmonic elimination pulse width modulation (SHEPWM) [9]. Since a PMSM is a multivariate close coupling, nonlinear, time-variable, symmetric parameter object and SVPWM have become the most prevalent PMSM modulation modes due to their three-phase symmetry, high direct voltage utilization rates, and low current ripple. The switching loss and cooling problems of a PMSM system tend to increase with raising in the power of the system and the DC-side voltage. These factors are the limitation of switching frequency. At a high speed in a PMSM, a low carrier wave and low switching frequency of the SVPWM lead to excessive current harmonics and higher switching loss. However, SHEPWM does not encounter this problem due to its low switching frequency and current harmonics. SHEPWM can eliminate selective harmonics by determining the Nth degree harmonic and fundamental waves, which improves the quality of the output wave and reduces the switching loss at high speeds [10], [11]. The switching angle in SHEPWM is the primary factor that determines the effect of the harmonic cancellation. SHEPWM with N switching angles can eliminate N-1 harmonics. Online computation can

Manuscript received Dec. 27, 2017; accepted Sep. 15, 2018

Recommended for publication by Associate Editor Dong-Hee Lee.

[†]Corresponding Author: guoxinhua@hqu.edu.cn

Tel: 159-8583-3956, Huaqiao University

^{*}Dept. of Electr. Eng., Col. Informat. Sci. & Eng., Huaqiao Univ., China

^{**}Xiamen EVADA Electronics Limited Corporation, China

guarantee the effect under different working conditions. However, an embedded system cannot ensure the timeliness and accuracy of data processing. Therefore, researchers often focus on the offline calculation of switching angle. The effects of this hybrid method can be summarized as follows.

1. Decreasing the switching frequency of an IGBT through the SHEPWM method since the switching frequency of SHEPWM was decided based on the frequency of the current and the number of switching angles which is far lower than that of SVPWM.
2. Compared to SVPWM, SHEPWM can reduce the harmonics of current when a PMSM works in the high speed condition and improves the efficiency of the PMSM system. In the high speed condition, the frequency of the current is higher than that in the low speed condition. Thus, the inductive and capacitive impedances are also higher than those in the low speed condition. Higher impedances mean a higher reactive loss which should be eliminated as much as possible in EV systems.
3. The modulation index M can be adjusted in every carrier wave cycle when the system is working under the SVPWM mode. However, when the system works under the SHEPWM mode, the M can only be adjusted in every fundamental current cycle which means that the response rate of SHEPWM is a lot slower than that of SVPWM especially in the low speed work condition. Thus, SVPWM and SHEPWM are used as modulation methods in order to achieve a rapid response of the system in the low speed work condition and lower current harmonics in the high speed work condition.

Most methods containing SHEPWM have been applied to two-level induction motors drive systems. Few articles have been published regarding the use of SHEPWM for three-level topology-based PMSMs.

Therefore, the hybrid modulation of SVPWM and SHEPWM is the highlight of PMSM drive system research. The authors of [12] analyzed the performance of SHEPWM and SVPWM for different frequencies. This analysis derived a relation between the harmonic characteristics and the ratio of the modulation and the carrier waves based on a two-level topology. However, the SVPWM was divided into an excessive number of sections, which hindered the algorithm implementation process under the high speed condition. The authors of [13] proposed a combination of SVPWM/ SHEPWM with a modulation strategy realized using an arbitrary time-switching method. In this strategy, the modulation methods were switched when the three-phase voltages for both of the modulations were the same. Unlike a two-level inverter, the three-phase voltage of a three-level inverter can be zero under the low-modulation condition. Under the influence of load torque, the motor speed decreases significantly for the three-phase all-in-zero condition. The working of a PMSM

cannot continue if the speed is reduced to zero, and the three-phase voltage is maintained at zero. The authors of [14], [15] proposed a PMSM modulation strategy and implementation method combined with synchronous SPWM, asynchronous SPWM and SHEPWM. However, in a PMSM drive system, the SVPWM performed better than the SPWM because of its three-phase symmetry.

This paper introduced hybrid methods into the three-level topology-based PMSMs, where previous methods have been applied to two-level induction motors drive systems. The proposed strategy used the switching angles (include the number and angle), stator current and rotation speed as feedback elements in a double closed-loop control strategy, which was used in an induction drive system. Furthermore, most three phase systems switch the modulations at the same time in order to reduce the impact of the harmonic current. However, they cannot totally avoid it. This paper chooses the phase current zero-crossing point as the switching point, which prevents the PMSM from being affected by harmonic current since in the phase current zero-crossing point, the amplitudes of the fundamental current and harmonic current are both zero.

The fundamental principle of SVPWM and mathematical models of a PMSM are discussed in Section II. A smooth switching method and the principle of SHEPWM for a PMSM are discussed in Section III. Simulation and experimental results are presented in Section IV. Some conclusions are drawn in Section V.

II. SVPWM FOR PMSMS

Fig. 1 shows the topology of a neutral-point-clamped three-level inverter in a PMSM system [16]. The inverter comprises two capacitors (C_1 and C_2), three bridges, each with four insulated gate bipolar transistor switches, and two clamped diodes. Each phase involves three types of switching states P, O and N. This three-level inverter has 27 output modes.

For convenience, a switch state S_i is equal to:

$$S_i = \begin{cases} P, & \text{if } S_{i1,2} \text{ on and } S_{i3,4} \text{ off} \\ O, & \text{if } S_{i2,3} \text{ on and } S_{i1,4} \text{ off} \\ N, & \text{if } S_{i3,4} \text{ on and } S_{i1,2} \text{ off} \end{cases}, (i = a, b, c) \quad (1)$$

Therefore, the phase voltage U_i is defined as:

$$U_i = S_i \frac{U_{dc}}{2}, (i = a, b, c) \quad (2)$$

Where U_a , U_b and U_c , represent the states of the three-phase output voltage of the inverter, and U_{dc} is the DC-link voltage.

Fig. 2 represents the corresponding 27 output modes of the three-level inverter space vector using a two-phase static coordinate system [17].

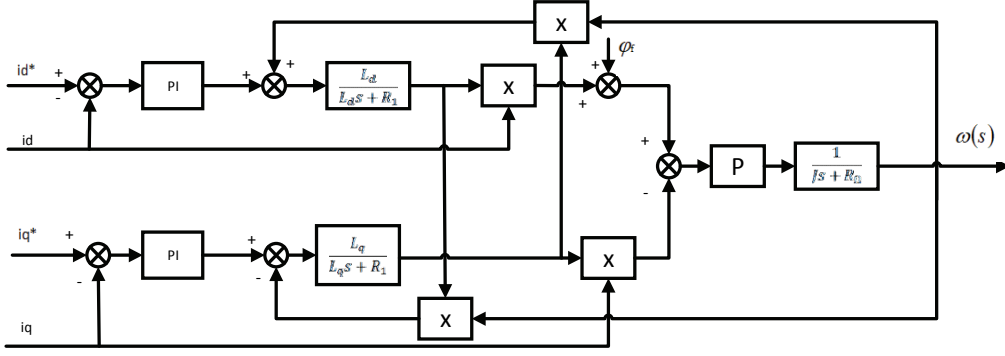


Fig. 3. PI closed loop transfer function block diagram for a PMSM.

In the PMSM control strategy, u_d and u_q were calculated using the difference between the field ($i_{d/q}^*$) current and the actual ($i_{d/q}$) current by using a proportional integral derivative (PID) algorithm in the inner current-loop. The flux linkage of the stator can be defined as follows:

$$\begin{cases} \psi_d = L_d i_d + \psi_f \\ \psi_q = L_q i_q \end{cases} \quad (9)$$

Where ψ_f is the permanent magnet flux, a constant determined by the properties of the permanent magnets. Therefore, equation (9) can be rewritten in the S-domain as:

$$\begin{cases} \psi_d = (u_d + \omega \psi_q) L_d / (L_d s + R_s) \\ \psi_q = (u_q + \omega \psi_d) L_q / (L_q s + R_s) \end{cases} \quad (10)$$

where R_s and ω are the stator resistor and the electrical angular velocity, respectively. $\omega(s)$ can be calculated using ψ_d and ψ_q . The transfer function model of a PMSM based on the proportional-integral algorithms is shown in Fig. 3.

According to equations (6)-(9), the state of a PMSM can be defined as follows:

$$\begin{bmatrix} \dot{i}_d \\ \dot{i}_q \\ \dot{\omega} \end{bmatrix} = \begin{bmatrix} -\frac{R_s}{L} & n_p & 0 \\ n_p & -\frac{R_s}{L} & -\frac{n_p \psi_f}{L} \\ 0 & \frac{n_p \psi_f}{L} & -\frac{B}{J} \end{bmatrix} \begin{bmatrix} i_d \\ i_q \\ \omega \end{bmatrix} + \begin{bmatrix} \frac{u_d}{L} \\ \frac{u_q}{L} \\ -\frac{T_L}{J} \end{bmatrix} \quad (11)$$

This study adapted the $i_d = 0$ control strategy to increase the efficiency of a PMSM system. A PMSM can reduce the reactive loss by using the $i_d = 0$ strategy. Equations (8) and (11) can be rewritten as follows:

$$T_e = \frac{3}{2} n_p \psi_f i_q \quad (12)$$

$$\begin{bmatrix} \dot{i}_q \\ \dot{\omega} \end{bmatrix} = \begin{bmatrix} -\frac{R_s}{L} & -\frac{n_p \psi_f}{J} \\ \frac{n_p \psi_f}{J} & 0 \end{bmatrix} \begin{bmatrix} i_q \\ \omega \end{bmatrix} + \begin{bmatrix} \frac{u_q}{L} \\ -\frac{T_L}{J} \end{bmatrix} \quad (13)$$

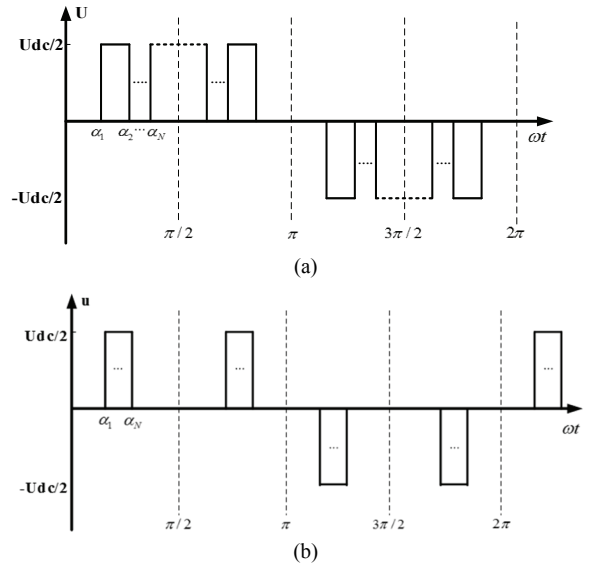


Fig. 4. Three-level inverter for a PMSM control system: (a) SHEPWM wave with odd angles; (b) SHEPWM wave with even angles.

III. SHEPWM AND HYBRID METHOD FOR A PMSM

The phase voltage of a three-level inverter was divided into unipolar and bipolar types. In this study, unipolarity was selected for SHEPWM because of the output mode of this topology [18]. Fig. 4 (a) and (b) show typical SHEPWM phase waveforms of a NPC three-level inverter. The SHEPWM of the three-level converter has N angles ($0 < \alpha_1 < \alpha_2 < \dots < \alpha_N < \pi/2$) in the first quarter period.

According to the Dirichlet rule, the Fourier series of the phase voltage can be defined as follows:

$$u(\omega t) = \sum_{n=1}^{\infty} [A_n \cos(n\omega t) + B_n \sin(n\omega t)] \quad n = 0, 1, 2, 3, \dots \quad (14)$$

$$A_n = \frac{1}{\pi} \int_0^{2\pi} u(\omega t) \cos(n\omega t) d(\omega t) \quad (15)$$

$$B_n = \frac{1}{\pi} \int_0^{2\pi} u(\omega t) \sin(n\omega t) d(\omega t) \quad (16)$$

The phase voltage $u(\omega t)$ is both an even-symmetry function between $\pi/2$ and $3\pi/2$, and an odd-symmetry function. Therefore, the phase voltage $u(\omega t)$ can be given as follows:

$$u(\omega t) = -u(\omega t + \pi) \quad (17)$$

$$u(\omega t) = u(\omega t - \pi) \quad (18)$$

Upon substituting equations (17) and (18) into (15) and (16), respectively, (15) and (16) can be rewritten as follows:

$$A_n = 0, n = 0, 1, 2, 3, \dots \quad (19)$$

$$B_n = \begin{cases} 0, n = 2, 4, 6, 8, \dots \\ \frac{2U_{dc}}{n\pi} \left[\sum_{k=1}^N (-1)^k \cos(n\alpha_k) \right], n = 1, 3, 5, 7, \dots \end{cases} \quad (20)$$

It is assumed that the entire harmonic wave has been eliminated, indicating that for $n = 1, 2, 3, \dots$, B_n is zero except for B_1 . The phase voltage U_a , U_b and U_c are defined as:

$$\begin{cases} U_a = B_1 \sin(\theta) \\ U_b = B_1 \sin(\theta - 120^\circ) \\ U_c = B_1 \sin(\theta + 120^\circ) \end{cases} \quad (21)$$

Substituting (21) into the formula for a Clarke transform, U_α and U_β can be defined as:

$$\begin{cases} U_\alpha = \sqrt{\frac{3}{2}} B_1 \sin \theta \\ U_\beta = -\sqrt{\frac{3}{2}} B_1 \cos \theta \end{cases} \quad (22)$$

Upon substituting (22) into (5), (5) can be rewritten as:

$$U_s = \sqrt{3} B_1 = \sqrt{U_\alpha^2 + U_\beta^2} \quad (23)$$

Similar to SVPWM, M is a constant with an amplitude between 0 and 1 due to the limitations of the voltage vector cycle. The modulation index M_{she} is defined as:

$$M_{she} = \frac{B_1}{U_{dc}/2} \quad (24)$$

Upon substituting (24) into (20), (20) can be rewritten as:

$$\begin{cases} B_1 = \frac{2U_{dc}}{\pi} \left[\sum_{k=1}^N (-1)^{k+1} \cos(\alpha_k) \right] = \frac{2}{3} M_{she} U_{dc} \\ B_n = \frac{2U_{dc}}{n\pi} \left[\sum_{k=1}^N (-1)^{k+1} \cos(n\alpha_k) \right] = 0 \end{cases} \quad (25)$$

The complete response of the stator current can be divided into the steady state response and the transient response, in order to keep the stator current distortion free during modulation switching, the transient response should be avoided. The complete response of the stator current can be defined as (26):

$$i_{a/b/c}(t) = \left[\frac{1}{L} e^{-\frac{Rs}{L+Lm}t} \int_0^\infty u_{a/b/c}(t) e^{\frac{Rs}{L+Lm}t} dt \right] + i_{a/b/c}(0_-) e^{-\frac{Rs}{L+Lm}t} \quad (26)$$

TABLE II
SIGNS OF THE HARMONIC CURRENTS WITH DIFFERENT ORDERS

| Nn | 1 | 2 | 3 | 4 | 5 |
|----|---|---|---|---|---|
| 5 | - | | | | |
| 7 | - | - | | | |
| 11 | + | + | + | | |
| 13 | - | + | + | + | |
| 17 | + | + | - | - | + |
| 19 | - | + | + | + | - |
| 23 | + | + | - | - | + |

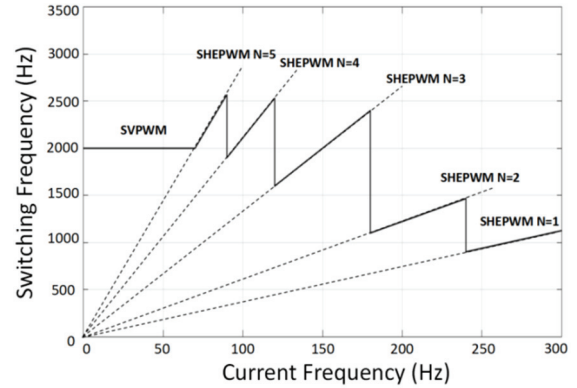


Fig. 5. Relation between the modulation and the switching frequency.

Where $i_{a/b/c}(t)$ is the complete response of the stator current, L , L_m and R_s are the equivalent self-inductor, mutual-inductor and equivalent resistance, respectively. In order to keep the current without distortion during modulation switching, $i_{a/b/c}(0_-)$ must be zero, which avoids the impact of the transient response. The amplitude of the harmonic current can be calculated using (26). The harmonic current exhibited different signs and amplitudes for different switching angles and modulation indices. Table II shows the sign of the harmonic current for $M_{she} = 0.6$.

Where n is the frequencies of the harmonic current, and N is the number of switching angles. As shown in Table II, the sign of the same frequency harmonic current under a different number of switching angles is sometimes disparate. For example, the sign of the 19th harmonic under $N=4$ differs from that figure under $N=5$. In addition, the amplitudes of the harmonic currents of the SVPWM, including the even and odd harmonics, are not zero. In order to prevent harmonic currents while switching the modulation between SVPWM and SHEPWM, switching points should be seriously considered.

This paper chooses the phase current zero-crossing point as its switching point. When the phase current is zero, the sign is irrelevant. This is due to the fact that in the phase current zero-crossing point, the amplitude of fundamental current and harmonic current are both zero. As for the switching point of SHEPWM with a different number of angles, the sign of the n -th harmonic current is varied.

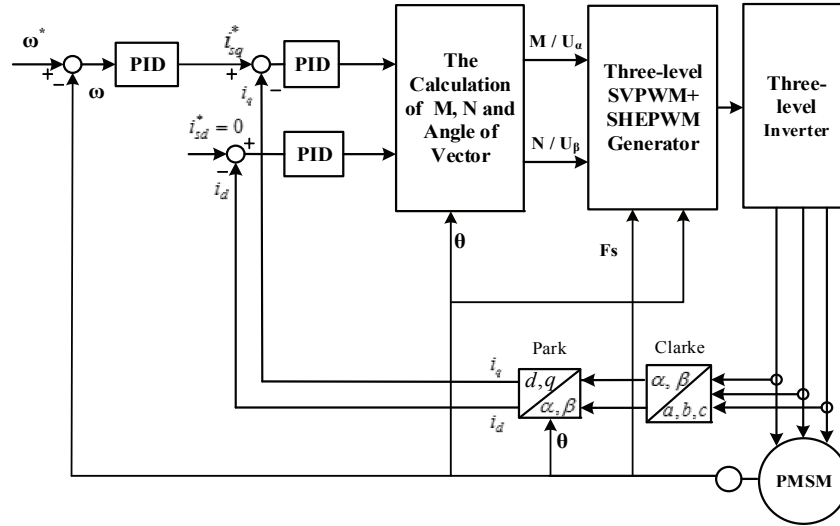


Fig. 6. Diagram of SVPWM + SHEPWM control system.

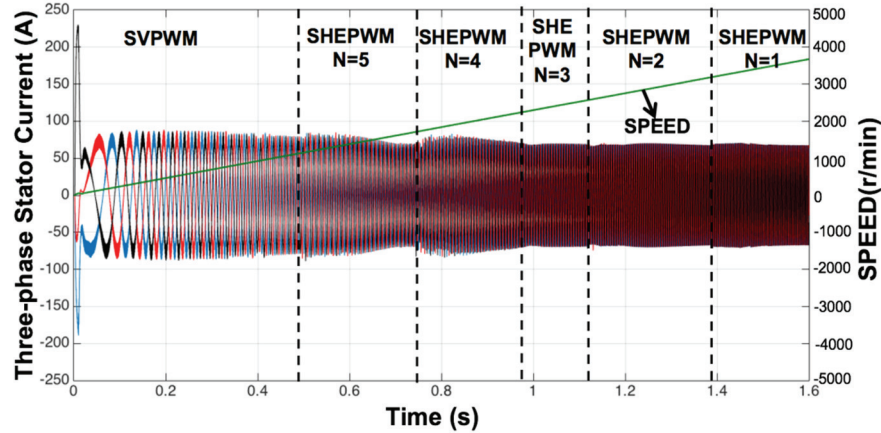


Fig. 7. Three phase stator current in different modulations and switching angles.

Fig. 5 summarizes the relation between the switching frequency and the motor speed (current frequency), which can be used to utilize modulations and to obtain the best performance of the PMSM.

When the control strategy is switched to SHEPWM, the switching frequency of a power device increased with the current frequency until the number of switching angles is changed.

IV. SIMULATION AND EXPERIMENTAL RESULTS

Fig. 6 shows a vector control system of a PMSM based on a maximum torque per ampere algorithm. The double-loop SVPWM/SHEPWM control mode was employed to obtain different motor speeds. The module calculated M and N under SHEPWM, and U_α and U_β under SVPWM for the PWM generation module. In order to prevent overshoot of the regulator, a limiter was added in the close-loop.

Simulation results of the three-phase stator currents are shown in Fig. 7, which include the current under different

modulation strategies. The current switching between different modulation strategies or modulation indices is smooth, as shown in Fig. 8. Simulation results show that the phase currents are kept distortion free while the modulations or switch angles change.

Fig. 9 shows simulation results of the fast Fourier transform (FFT) analyses under different modulation strategies and indices. The simulation results show that SHEPWM with N switching angles can eliminate harmonic current of the order $N-1$.

Fig. 10(a) shows experimental results of the line voltage when the modulation strategies were switched. Fig. 10(b) shows simulation result of the line voltage when the number of switching angles is changed from 5 to 4.

Fig. 11 shows simulations of the D-axis current and Q-axis current of a PMSM. Fig. 12 show the simulation speed and torque of a PMSM. When $t=2.8s$, there is a load variation. The simulation results show that the D/Q-axis currents and torque did not change a lot when the modulations or switch angles changed. The speed reached the rated value again in 2

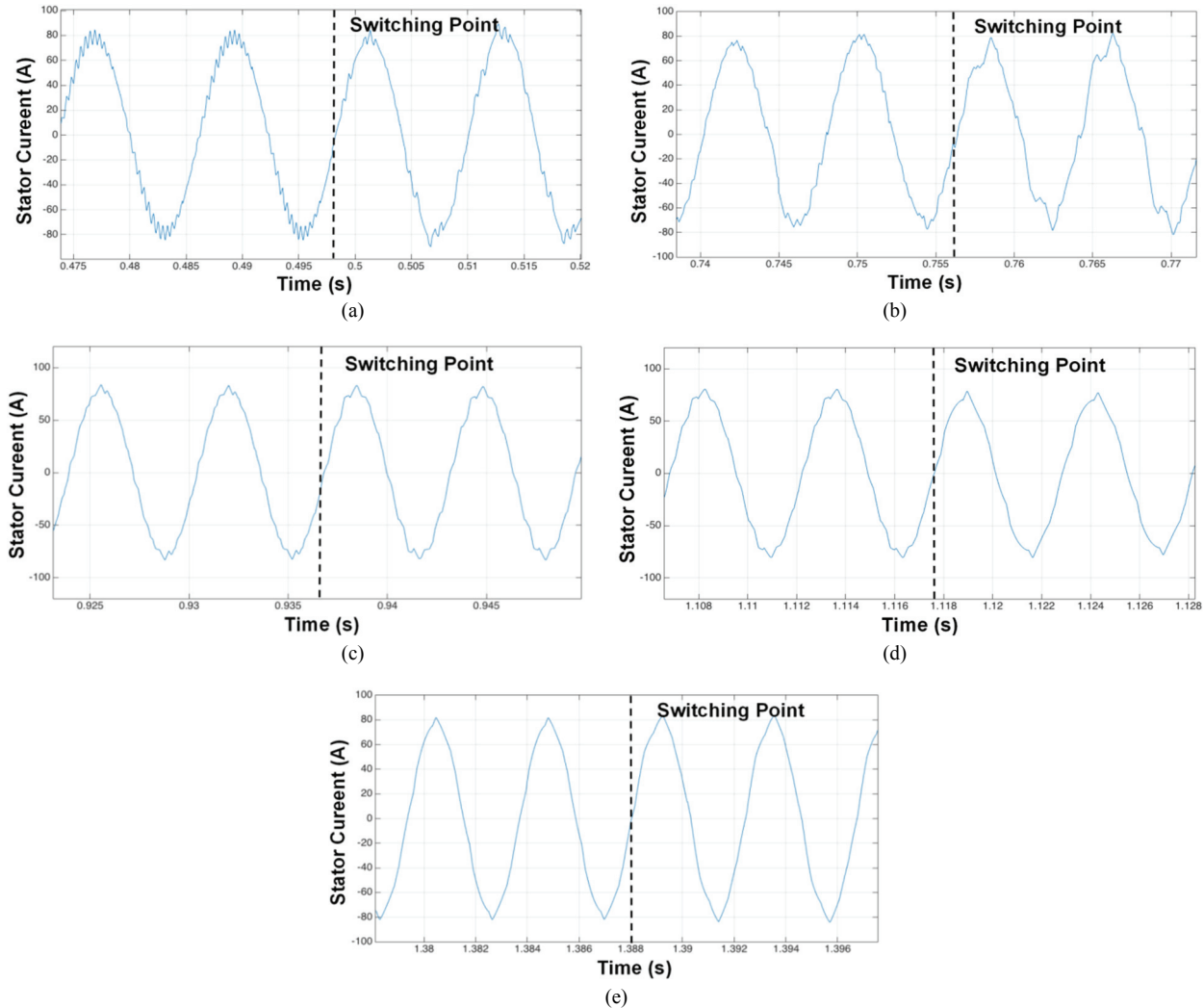


Fig. 8. Simulated current under different conditions: (a) Simulated current wave during a transition between SVPWM and SHEPWM with $N = 5$; (b) Simulated current wave during a transition between SHEPWM with $N = 5$ and SHEPWM with $N = 4$; (c) Simulated current wave during a transition between SHEPWM with $N = 4$ and SHEPWM with $N = 3$; (d) Simulated current wave during a transition between SHEPWM with $N = 3$ and SHEPWM with $N = 2$; (e) Simulated current wave during a transition between SHEPWM with $N = 2$ and SHEPWM with $N = 1$.

seconds, while a load variation was added in 2.8s. Fig. 13 show the neutral voltage difference during a load variation, which was achieved by a DC source (three-level rectifier).

Fig. 14 and 15 show the simulation results of three phase currents and FFT analysis under SVPWM mode in high speed condition. The simulation result shows that current harmonic distortions was 7.52% under SVPWM while that figure under SHPWM was 4% approximately in same speed.

Fig. 16 and 17 show the PMSM and test device comprising a three-level inverter and the control system of the PMSM.

Experimental results of the stator currents and the d/q-axis currents are shown in Fig. 18 and 19. The experiment involved the study of current under different modulation strategies and switching angles. For the SHEPWM with $N = 4$, the frequency of the stator current reached 120 Hz, indicating that the motor speed reached 1500 rotations per minute. The

motor speed of this PMSM system was approaching its limits. Due to the limitation of the objective condition, the experimental results are partially complete for SVPWM and SHEPWM with $N = 5$ and $N = 4$, respectively. The experimental results show that the hybrid modulation of the PMSM can provide a smooth and stable current transition and harmonic elimination.

Fig. 20 shows experimental results of FFT analyses under different modulation strategies and indices. The experimental results indicate that SHEPWM with N can eliminate harmonic current of the order $N-1$. The total harmonic distortions of the three styles (SVPWM, SHEPWM for $N=5$ and SHEPWM for $N=4$) were 11.54%, 9.65% and 10.12%, respectively.

Fig. 21 and Fig. 22 show the experimental torque and speed under different modulation strategies and switching

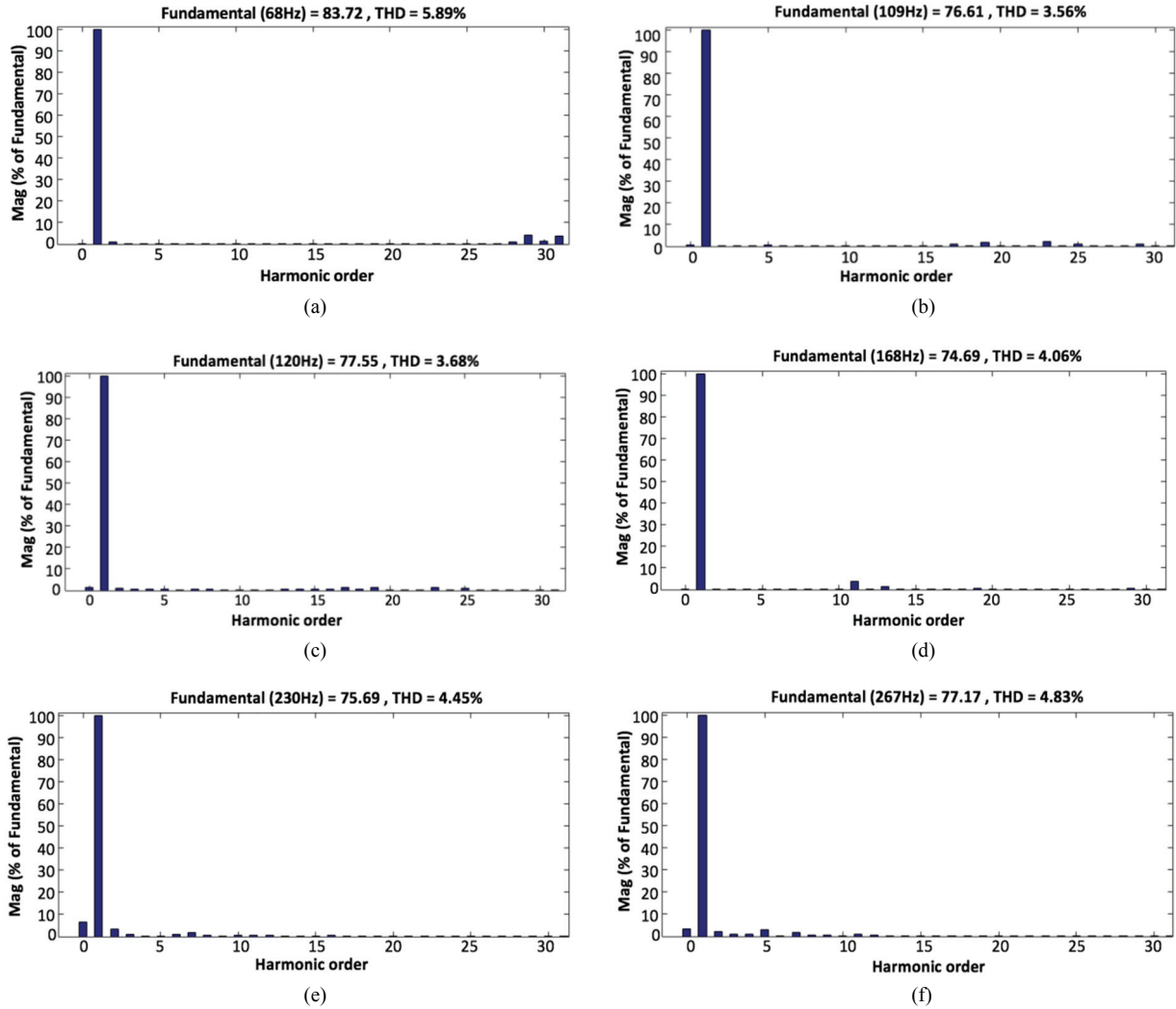


Fig. 9. FFT results under different conditions: (a) FFT result with SVPWM; (b) FFT result with SHEPWM for $N = 5$; (c) FFT result with SHEPWM for $N = 4$; (d) FFT result with SHEPWM for $N = 3$; (e) FFT result with SHEPWM for $N = 2$; (f) FFT result with SHEPWM for $N = 1$.

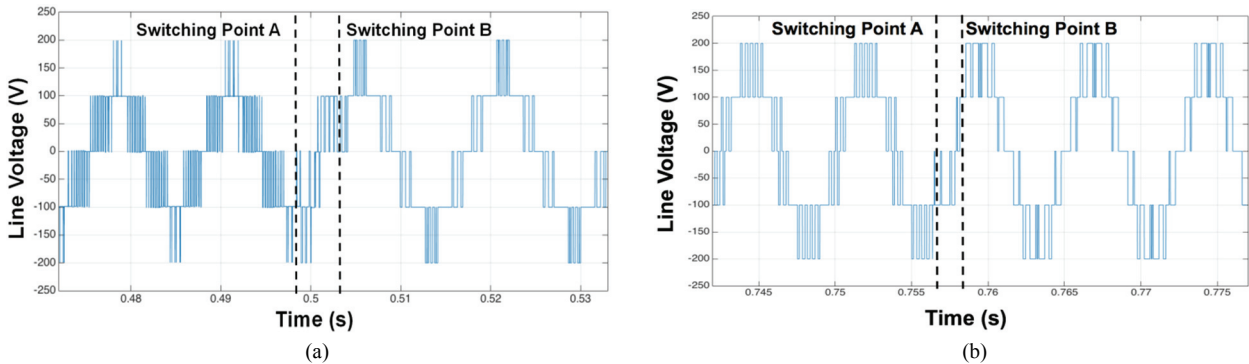


Fig. 10. Simulated line voltage during transitions between different conditions: (a) Simulated result of a line voltage wave during a transition between SVPWM and SHEPWM $N = 5$; (b) Simulated result of a line voltage wave during a transition between SHEPWM $N = 5$ and SHEPWM with $N = 4$.

angles. These results show that speed and torque are kept distortion free while the modulations or switch angles change.

Fig. 23 shows experimental result of the line voltage during

a switching of the modulation strategies. Fig. 24 shows experimental result of the line voltage when the number of switching angles is changed.

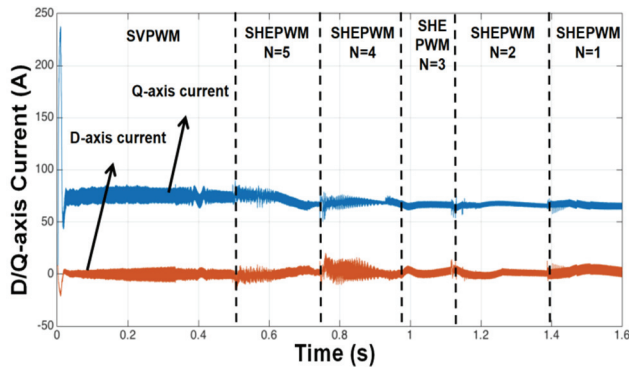


Fig. 11. Simulation D/Q-axis current of a PMSM.

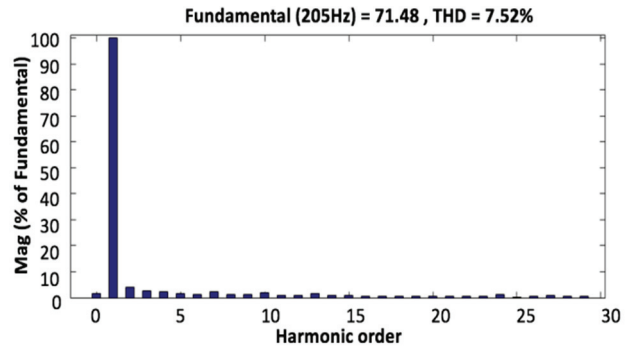


Fig. 15. FFT results of the current with SVPWM.

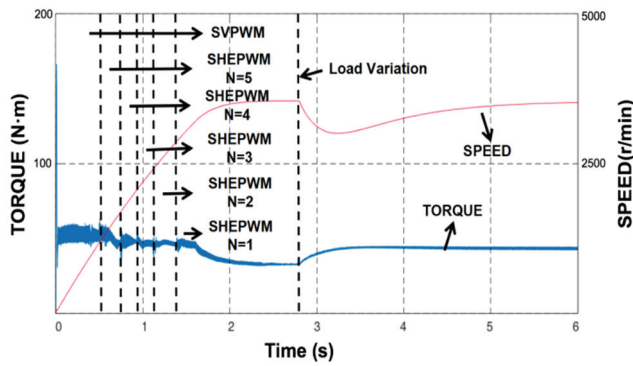


Fig. 12. Simulation result of the speed and torque of a PMSM.

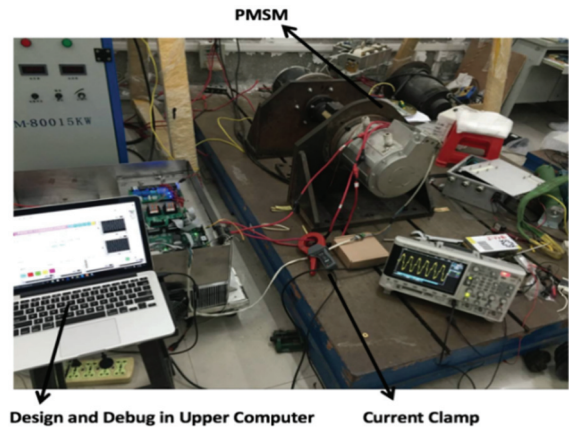


Fig. 16. PMSM drive system based on the three-level topology.

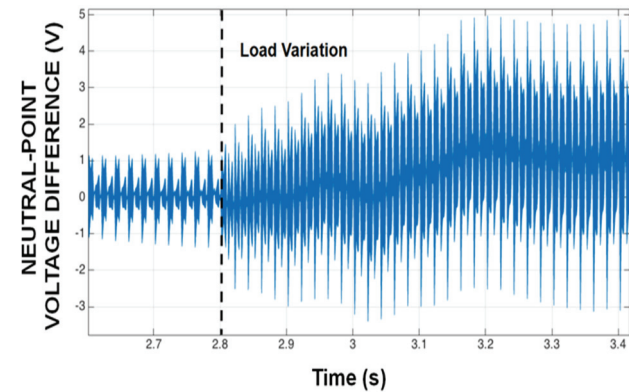


Fig. 13. Neutral-point voltage difference when the load changes.

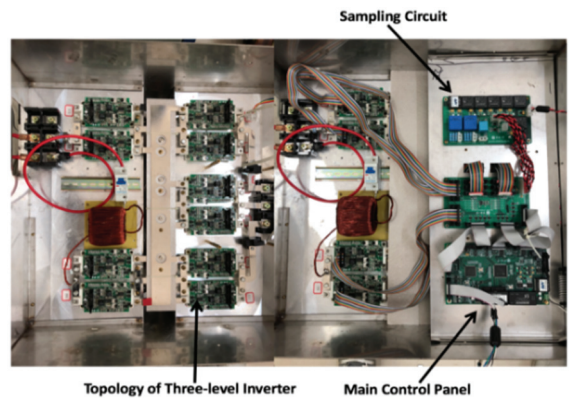


Fig. 17. Three-level topology and PMSM controller.

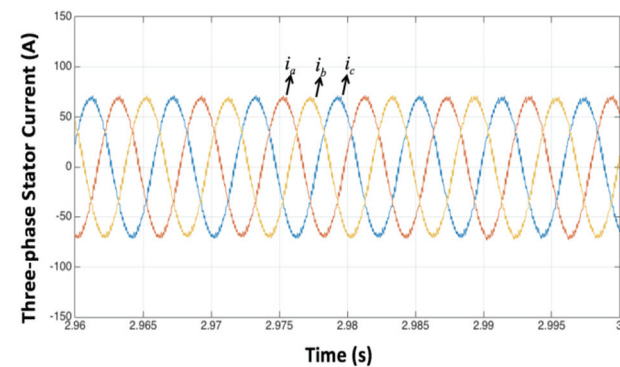


Fig. 14. Three phase stator current under the SVPWM mode.

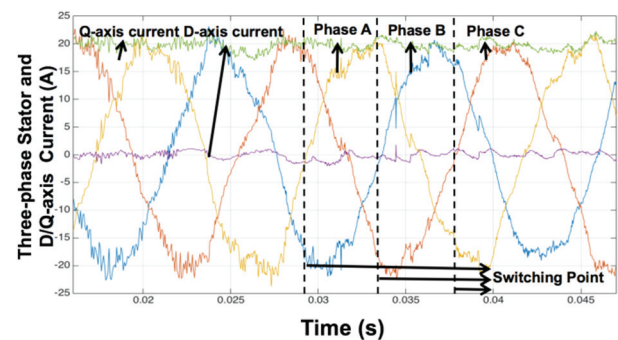


Fig. 18. Experimental current wave during a transition between SVPWM and SHEPWM.

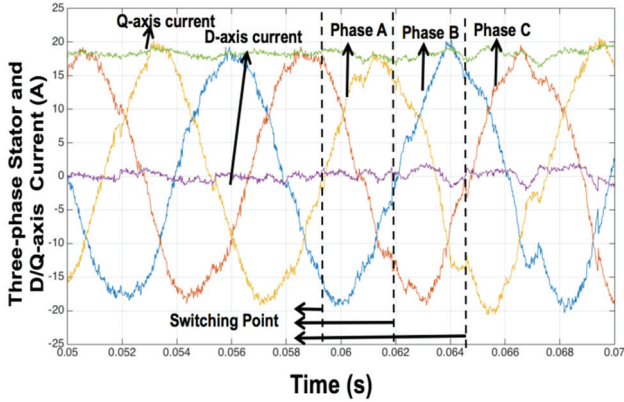


Fig. 19. Experimental current wave during a transition between SHEPWM with $N = 5$ and SHEPWM $N = 4$.

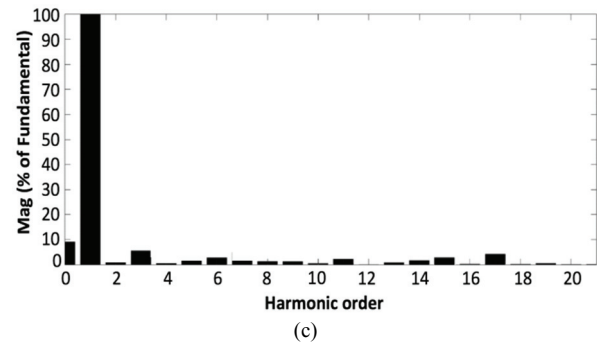
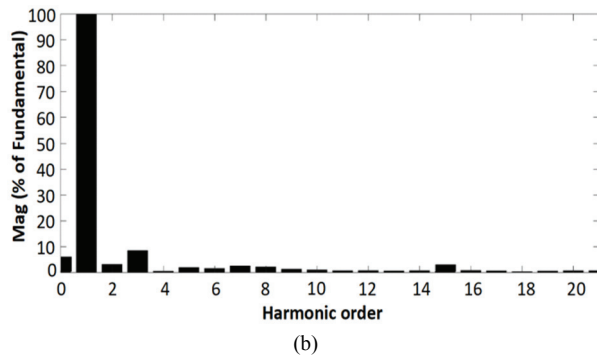
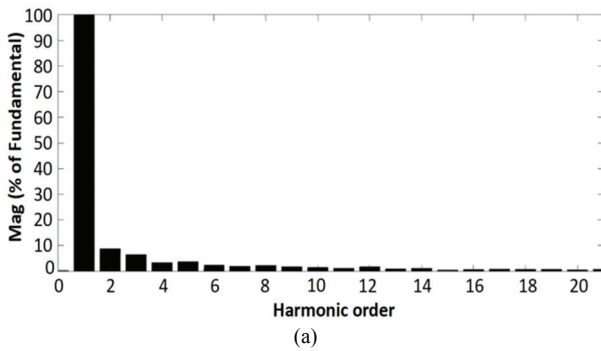


Fig. 20. FFT results of experimental current: (a) FFT result with SVPWM (experiment); (b) FFT result with SHEPWM for $N = 5$ (experiment); (c) FFT result with SHEPWM for $N = 4$ (experiment).

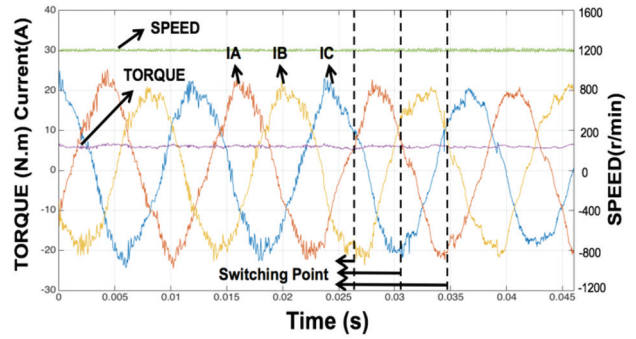


Fig. 21. Experimental torque and speed during a transition between SVPWM and SHEPWM with $N = 5$.

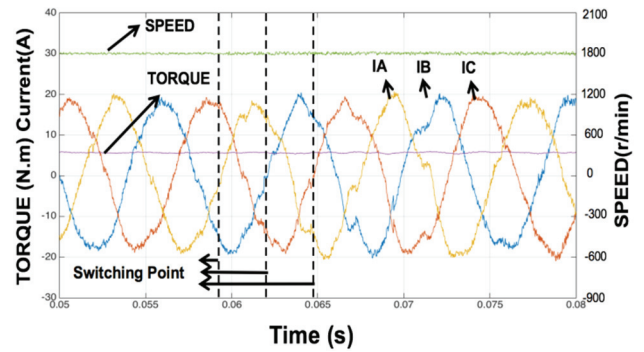


Fig. 22. Experimental torque and speed during a transition between SHEPWM with $N = 5$ and SHEPWM with $N = 4$.

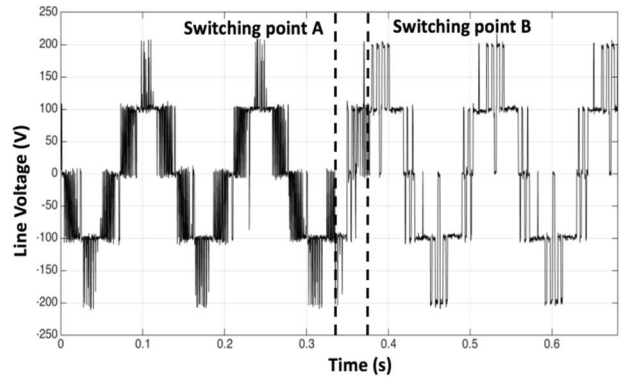


Fig. 23. Experimental line voltage waves during a transition between SVPWM and SHEPWM with $N = 5$.

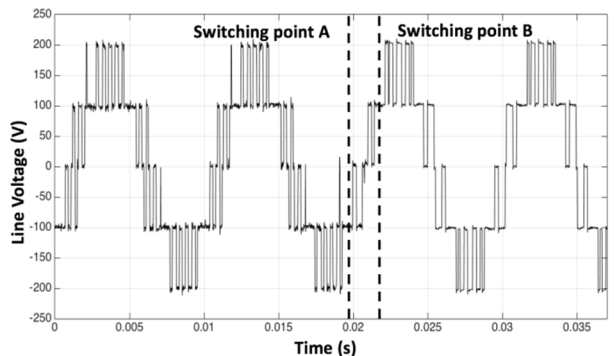


Fig. 24. Experimental line voltage waves during a transition between SHEPWM with $N = 5$ and SHEPWM with $N = 4$.

V. CONCLUSIONS

This paper proposed a hybrid method that includes SVPWM and SHEPWM for the three-level inverters in PMSM drive systems in order to satisfy the demands of a quick response in the low-speed condition and a low harmonic current in the high-speed condition. The method introduced a smooth current transition for the SHEPWM with different numbers of switch angles and modulations strategies, which using the phase current zero-crossing point as their switching points.

Simulation and experimental results confirmed the effectiveness of the proposed method for selective harmonic elimination in the high-speed condition and a smooth transition of the current. They also show that the proposed method can ensure that the speed, id , iq and torque are kept distortion free while the modulations or switch angles are changed.

ACKNOWLEDGMENT

This work was supported in part by the National Natural Science Foundation of China under Project (51477058 and 51707068), the Science and Technology Planning Project of Fujian Province under Project (2017H0021 and 2017J01097), the Promotion Program for Young and Middle-aged Teacher in Science and Technology Research of Huaqiao University under Project (ZNQ-YX304) and the Opening Foundation of key Laboratory of Power Electronic Drive, Chinese Academy.

REFERENCES

- [1] G. I. Orfanoudakis, M. A. Yuratich, and S. M. Sharkh, "Analysis of dc-link capacitor current in three-level neutral point clamped and cascaded H-bridge inverters," *IET Power Electron.*, Vol. 6, No. 7, pp. 1376-1389, Sep. 2013.
- [2] V. Michal, "Three-level PWM floating H-bridge sinewave power inverter for high-voltage and high-efficiency applications," *IEEE Trans. Power Electron.*, Vol. 31, No. 6, pp. 4065-4074, Jun. 2016.
- [3] J. Y. Xue, X. H. Guo, S. L. Li, J. Y. Fu, R. M. Fang, and Z. S. Li, "The SVPWM and PR control for single-phase three-level rectifier," *20th International Conference on Electrical Machines and Systems*, pp. 1-6, Oct. 2017.
- [4] X. H. Zhang and W. K. Yue, "Neutral point potential balance algorithm for three-level NPC inverter based on SHEPWM," *Electron. Lett.*, Vol. 53, No.23, pp. 1542-1544, Nov. 2017.
- [5] K. Ma and F. Blaabjerg, "Modulation methods for three-level neutral-point-clamped inverter achieving stress redistribution under moderate modulation index," *IEEE Trans. Power Electron.*, Vol. 31, No. 1, pp. 5-10, Jan. 2016.
- [6] A. Abdelhakim, P. Mattavelli, and G. Spiazzi, "Three-phase three-level flying capacitors split-source inverters: Analysis and modulation," *IEEE Trans. Ind. Electron.*, Vol. 64, No. 6, pp. 4571-4580, Jun. 2016.
- [7] K. Antoniewicz, M. Jasinski, M. P. Kazmierkowski, and M. Malinowski, "Model predictive control for three-level four-leg flying capacitor converter operating as shunt active power filter," *IEEE Trans. Ind. Electron.*, Vol. 63, No. 8, pp. 5255-5262, Aug. 2016.
- [8] X. Q. Wang, Z. Wang, M. Cheng, and Y. H. Hu, "Remedial strategies of T-NPC three-level asymmetric six-phase PMSM drives based on SVM-DTC," *IEEE Trans. Ind. Electron.*, Vol. 64, No. 9, pp. 6841-6853, Mar. 2017.
- [9] Y. X. Chen, X. H. Guo, S. D. Li, J. Y. Fu, R. M. Fang, and Z. S. Li, "Design of three-level inverter in permanent magnet synchronous motor system based on repetitive control," *20th International Conference on Electrical Machines and Systems*, pp.1-6, Oct. 2017.
- [10] Y. Wang, X. Wen, and F. Zhao, "Vector control of six-phase PMSMs with selective harmonic elimination PWM," *Transport. Electrification. Asia-Pacific*, pp. 1-6, Oct. 2014.
- [11] R. Salehi, N. Farokhnia, M. Abedi, and S. H. Fathi, "Elimination of low order harmonics in multilevel inverters using genetic algorithm," *J. Power Electron.*, Vol. 11, No. 2 pp. 132-139, Mar. 2011.
- [12] K. Wang, X. J. You, C. C. Wang, and M. L. Zhou, "Research on the comparison of synchronized modulation of SHEPWM and SVPWM under low switching frequency," *Trans. China Electrotechnical Society*, Vol. 30, No. 14, pp. 333-341, Jul. 2015.
- [13] Z. G. Zhang, S. D. Huang, C. G. Hu, and W. J. Zhang, "Hybrid method of three-level SHEPWM and SVPWM and its vector smooth-switching," *Trans. China Electrotechnical Society*, Vol. 30, No. 14, pp. 342-349, Jul. 2015.
- [14] X. H. Guo, Y. X. Wang, F. Zhao, and X. H. Wen, "Two level control technology of PMSM used in medium voltage high power traction system based on SHEPWM," *Trans. China Electrotechnical Society*, Vol. 27, No. 11, pp. 76-82, Nov. 2012.
- [15] Y. X. Wang, X. H. Wen, F. Zhao, and X. H. Guo, "Selective harmonic elimination PWM technology applied in PMSMs," *IEEE Vehicle Power and Propulsion Conference*, pp. 92-97, Oct. 2012.
- [16] Z. Wang, Y. B. Wang, J. Chen, and M. Cheng, "Fault tolerant control of NPC three-level inverters fed double-stator-winding PMSM drives based on vector space decomposition," *IEEE Trans. Ind. Electron.*, Vol. 64, No. 11, pp. 8446-8458, Nov. 2017.
- [17] J. H. Seo, H. C. Chang, and S. H. Dong, "A new simplified space-vector PWM method for three-level inverters," *IEEE Trans. Power Electron.*, Vol. 16, No. 4, pp. 545-550, Jul. 2001.
- [18] C. G. Hu, G. Holmes, W. X. Shen, X. H. Yu, Q. J. Wang, and F. L. Luo, "Neutral-point potential balancing control strategy of three-level active NPC inverter based on SHEPWM," *IET Power Electron.*, Vol. 10, No. 14, pp. 1943-1950, Nov. 2017.



Yuanxi Chen was born in Fujian, China. He received his B.S. degree in Electronic Science and Technology, and his M.S. degree Electrical Engineering from Huaqiao University, Fujian, China, in 2015 and 2018, respectively. His current research interests include PMSM drives and multiple-level inverter control.



Jiangyu Xue was born in Fujian, China. He received his B.S. degree in Electrical Engineering from the Fujian Agriculture and Forestry University, Fujian, China, in 2015; and his M.S. degree in Electrical Engineering from Huaqiao University, Fujian, China, in 2018. His current research interests include power converters.



Xinhua Guo was born in Fujian, China. He graduated from Nanjing Institute of Technology in 2000. He received his M.S. degree in Agricultural Electrification and Automation from Jiangsu University, Jiangsu, China, in 2006; and his Ph.D. degree in Electrical Engineering from the Institute of Electrical Engineering (IEE), Chinese Academy of Sciences (CAS), Beijing, China, in 2010. He is presently working as an Associate Professor at Huaqiao University, Xiamen, China, and at the Fujian Engineering Research Center of Motor Control and System Optimal Schedule, Xiamen, China. Before that, he was a Research Assistant in IEE, CAS. In addition, he worked for TDK from July 2000 to August 2004. His current research interests include IGBT packaging technology, PMSMs and their drive control for EVs, and special motors and their drive control.



Yifeng Chen was born in Fujian, China. He received his B.S. degree in Electronics and Communication Engineering in the Department of Radio Engineering, Shandong University, Shandong, China, in 1988. He is presently working as the Chief Technology Officer of Xiamen EVADA Electronics Limited Corporation and is the Standing Director of the Fujian Power Supply Society. His current research interests include modular power supply control, UPS and PV grid-connected inverters.